HIGH STRAIN RATE BEHAVIOUR OF AN AZ31 + 0.5 Ca MAGNESIUM ALLOY

Zuzanka Trojanová[1,*], Pavel Lukáč[1], Tomáš Podrábský[2], Josef Pešička[1]

[1]Department of Physics of Materials, Faculty of Mathematics and Physics, Charles University in Prague, Ke Karlovu 5, 121 16 Praha 2, Czech Republic
[2]Istitute of Materials Science and Engineering, Faculty of Mechanical Engineering, Brno University of Technology, Technická 2896/2, CZ-616 69 Brno, Czech Republic
[*]Corresponding author, e-mail address: ztrojan@met.mff.cuni.cz

Resume

The paper reports behaviour of magnesium alloy AZ31 (nominal composition 3 % Al - 1 % Zn – balance Mg) with an addition of 0.5 wt. % Ca at high strain rates. Samples were prepared by the squeeze cast technology. Dynamic compression Hopkinson tests were performed at room temperature with impact velocities ranging from 11.2 to 21.9 $m.s^{-1}$. A rapid increase of the flow stress and the strain rate sensitivity was observed at high strain rates. Transmission electron microscopy showed extremely high dislocation density and mechanical twins of two types. Adiabatic shear banding is discussed as the reason for the observed behaviour at high strain rates.

Available online: http://fstroj.uniza.sk/journal-mi/PDF/2012/02-2012.pdf

Article info

Article history:
Received 6 August 2011
Accepted 10 October 2011
Online 27 November 2011

Keywords:
Mechanical Properties;
Magnesium Alloy;
High Strain Rates;
Dislocations;
Mechanical Twins

ISSN 1335-0803 (print version)
ISSN 1338-6174 (online version)

1. Introduction

The strength of many metallic materials increases with increasing strain rate and decreases with increasing temperature. This behaviour is explained by thermally activated dislocation motion and interaction between dislocations and solute atoms. When temperature increases, there is more thermal energy available for dislocation motion, whereas when the strain rate increases the time necessary for overcoming of local obstacles in the slip plane is shorter. At low temperature and low and intermediate strain rates the deformation process is approximately isothermal. At higher strain rates, thermal conditions gradually change to adiabatic and the internal temperature of the sample increases. Then the deformation temperature is higher than ambient temperature. The strain hardening in magnesium alloys, i.e. increase of dislocation density during deformation, can be modified by mechanical twinning. Twins may contribute to straining but on the other hand, small twins are obstacles for dislocation motion; they contribute to the hardening. The high strain rate behaviour of metallic materials has been reported in various papers [1-4]. Recently, the critical review of high strain rate properties was done by Armstrong and Walley [5]. At high strain rates some critical strain rate exists at which the thermally activated rate controlling mechanism changes to viscous phonon drag [6]. Zerilli and Armstrong modified this idea including the dislocation drag into the model of thermal activation [7].

Mg-Al-Zn alloys offer good combination of the room temperature strength and ductility, good salt spray corrosion resistance and excellent die castability. They have been widely used in the automotive and electronic industries [8]. However, all applications of these alloys are limited to components

operating at temperatures lower than 400 K because of their rapid strength reduction at higher temperatures. In order to overcome this disadvantage, Ca - containing Mg alloys were developed with the aim to improve mechanical properties at elevated temperature. Ca is cheap and light alloying element [9]. Additionally, the Ca addition to magnesium alloys improves the creep resistance at elevated temperatures [10, 11]. The addition of Ca can refine the grain size, disperse the particle and break down the dendritic morphology of particle into round and well distributed small particles [8].

The objective of this work is to investigate the deformation behaviour of an AZ31 alloy with Ca addition in dynamic experiments at various strain rates.

2. Experimental procedure

0.5 wt. % of calcium was added to the commercial Mg alloy AZ31 (nominal composition: 3%Al, 1%Zn, balance Mg). The material was prepared using the squeeze casting technology. Cylindrical specimens of 9 mm diameter and 9 mm length were machined from the cast discs. The dynamic compression experiments were performed using split Hopkinson pressure bar (SHPB) technique. The SHPB test is the most commonly used method for determining material properties at high strain rates. The split Hopkinson bar apparatus consists of two long slender bars that sandwich a short cylindrical specimen between them. By striking the end of a bar, a compressive stress wave is generated that immediately begins to traverse towards the specimen. Upon arrival at the specimen, the wave partially reflects back towards the impact end. The remainder of the wave transmits through the specimen and into the second bar causing irreversible plastic deformation in the specimen. It is shown that the reflected and transmitted waves are proportional to the specimen's strain rate and stress, respectively. Specimen strain can be determined by integrating the strain rate. By monitoring the strains in the two bars, specimen stress-strain properties can be calculated. The stress is done by

$$\sigma(t)=\frac{ES_{bar}}{2S_{sam}}\left[\varepsilon_i(t)+\varepsilon_r(t)+\varepsilon_t(t)\right] \qquad (1)$$

and

$$\varepsilon(t)=\frac{C_0}{L_{sam}}\int_0^t\left[\varepsilon_i(t)-\varepsilon_r(t)-\varepsilon_t(t)\right], \qquad (2)$$

where $\varepsilon_i(t)$, $\varepsilon_r(t)$, $\varepsilon_t(t)$ are incident, reflected and transmitted axial strains. Correspondent strain and strain rate can be calculated as

$$\dot{\varepsilon}(t)=\frac{C_0}{L_{sam}}\left[\varepsilon_i(t)-\varepsilon_r(t)-\varepsilon_r(t)\right]. \qquad (3)$$

In equation (3) E is the elastic modulus of bars, S_{bar}, S_{sam} are cross–sections of bar or sample, L_{sam} length of sample and C_0 sound velocity. HSBP tests were performed at temperature of 28.5 °C. For comparison quasi-static compression experiments at a strain rate of $8.3\text{x}10^{-3}$ s^{-1} were performed. The activation volume was estimated in the stress relaxation test. Transmission electron microscopy (TEM) investigations were performed with a Jeol 2000 FX electron microscope operated at 200 kV.

3. Experimental results and discussion

Transmission electron micrograph of the as prepared alloy is introduced in Fig. 1.

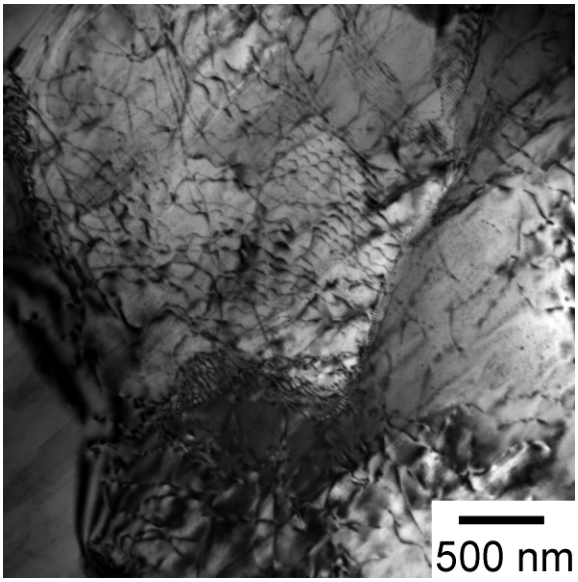

Fig. 1. TEM micrograph of the as prepared alloy

Relatively high dislocation density is a characteristic feature of this state. Segments of the dislocation network are visible in Fig. 1. It is a consequence of the squeeze cast technique used for the preparation of the material. Engineering stress-strain curves obtained for various impact velocities are introduced in Fig. 2 for various impact velocities.

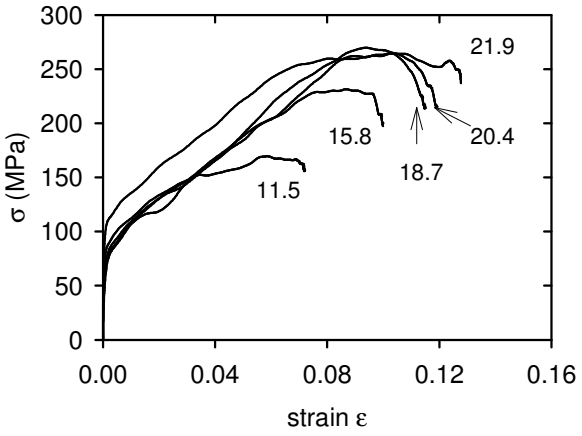

Fig. 2. Engineering stress-strain curves obtained for various impact velocities (in ms^{-})

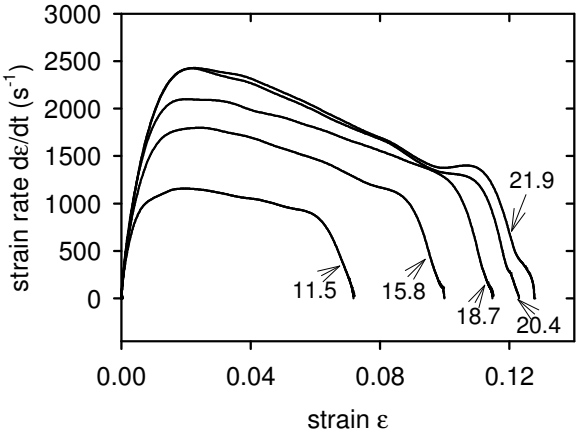

Fig. 3. Strain rate as a function of strain for various impact velocities (in ms^{-1})

The strains dependences of the strain rate given in Fig. 3 were estimated for various impact velocities. The strain rate increases with increasing strain approaching its maximum value at a strain of approximately 0.02.

The strain rate dependence of the yield stress is introduced in Fig. 4. Rapid increase of the strain rate sensitivity at high strain rates can be seen from Fig. 4. It should be note that each experiment at higher strain rates was performed several times. Values of the yield stress introduced in Fig. 4 are the mean values. The maximum strain rate dependence of the elongation to fracture ε_f is introduced in Fig. 5. Similarly as in the case of the yield stress the values of the fracture strain are the mean values estimated form the several experiments. Comparing with ductility estimated in the quasi−static experiment at room temperature, the fracture strain decreases, but in the high strain rate region it increases again with an increase in the strain rate.

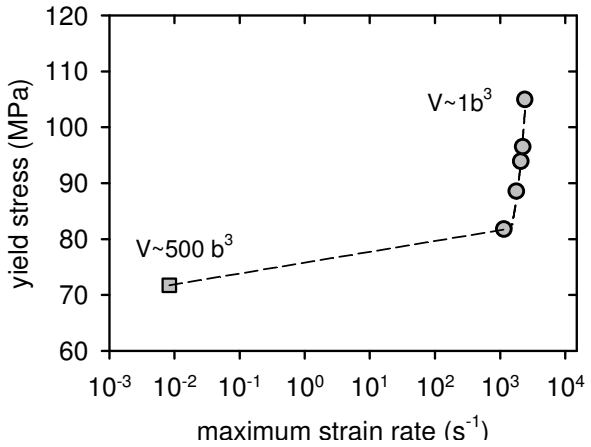

Fig. 4. Strain rate dependence of the yield stress

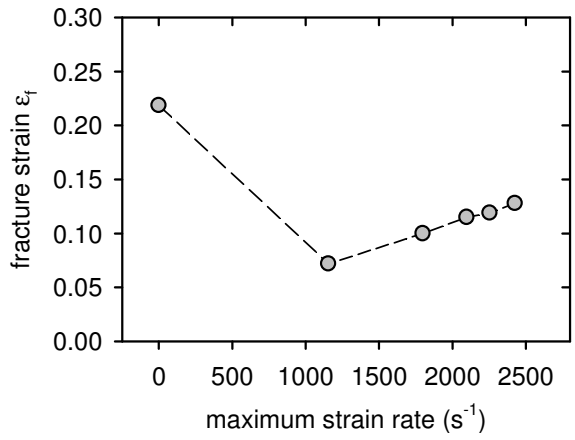

Fig. 5. Strain rate dependence of the fracture strain

3.1 Thermal activation

The strain rate, $\dot{\varepsilon}$, and temperature, T, dependence of the flow stress, σ, depends on the

dislocation rate controlling deformation mechanism. Usually this dependence is described by the Arrhenius equation:

$$\dot{\varepsilon} = \dot{\varepsilon}_0 \exp\left(-\frac{\Delta G}{k_B T}\right) , \quad (4)$$

where $\dot{\varepsilon}_0$ is the pre-exponential term, ΔG the Gibbs free enthalpy depending on the thermal (effective) stress $\sigma^* = \sigma - \sigma_i$ (σ_i is the internal stress). Kocks et al. [6] found the following empirical relationship for this dependence

$$\Delta G = \Delta G_0 \left[1 - \left(\frac{\sigma^*}{\sigma_0^*}\right)^p\right]^q . \quad (5)$$

Model parameters p and q describe the statistical shape of the local obstacle profile. ΔG_0 is the Gibbs free enthalpy necessary for overcoming a short range obstacle without the stress and σ_0^* is the thermal stress at 0 K.

The activation volume is defined as

$$V = \frac{\partial \Delta G}{\partial \sigma^*} = k_B T \frac{\partial \ln \dot{\varepsilon} / \dot{\varepsilon}_0}{\partial \sigma^*} \quad (6)$$

and substituting from (5), we obtain

$$V = \frac{\Delta G_0 pq}{\sigma_0^*}\left[1 - \left(\frac{\sigma^*}{\sigma_0^*}\right)^p\right]^{q-1}\left(\frac{\sigma^*}{\sigma_0^*}\right)^{p-1} . \quad (7)$$

Two sets of values are typically used [7]. The set $p = q = 1$ corresponds to a "rectangular" obstacle profile and a regular lattice arrangement of obstacles and leads to a constant activation volume $V = m.kT/\sigma^*$. The set $p = 1/2$ and $q = 3/2$ corresponds to a more realistic obstacle shape and distribution. Geometrically, the activation volume $V = b.d.L$, where d is the obstacle width and L is the mean length of dislocation segments between obstacles. The strain rate sensitivity parameter

$m^* = \left(\frac{\partial \ln \sigma^*}{\partial \ln \dot{\varepsilon}}\right)_{T,\varepsilon}$ is often defined by its inverse, the stress sensitivity parameter m

$$m^{*-1} = m = \left(\frac{\partial \ln \dot{\varepsilon}}{\partial \ln \sigma^*}\right)_{T,\varepsilon} = \frac{\Delta G_{0pq}}{k_B T}\left[1 - \left(\frac{\sigma^*}{\sigma_0^*}\right)^p\right]^{q-1}\left(\frac{\sigma^*}{\sigma_0^*}\right)^p \quad (8)$$

Rapid increase of the strain rate sensitivity at higher strain rates is obvious from Fig. 3. Similar dependence was observed also in fcc metals (see for example [8]). The activation volume estimated at higher strain rates exhibits very small values, approximately $V \sim b^3$, where b is the Burgers vector of dislocations. The value of the activation volume estimated at room temperature in the quasi–static experiment in the vicinity of the yield stress was $V \sim 500b^3$. The limiting small value of the activation volume estimated at high strain rates and rapid increase of the flow stress indicate a change in deformation mechanism. One possibility how to explain this behaviour is to consider the transition from thermal activation to drag-controlled deformation that occurs when a constant structure is subjected to increasing stresses or strain rates. Zerilli and Armstrong [9] proposed a new model introducing the dislocation drag into the model of the thermal activation. They estimated that the dislocation drag may significantly change the strain rate dependence of the flow stress. From the results by Zerilli and Armstrong, it may be concluded that the dislocation drag at the strain rates in the order 10^3 s^{-1} has only marginal influence. The strong upturn observed for the flow stress is not caused by the dislocation drag.

3.2. Adiabatic shear banding

The mean velocity of dislocations v is connected with the plastic strain rate by the Orowan equation

$$\dot{\varepsilon} = (1/\psi)\rho_m b v \quad (9)$$

where ρ_m is the density of mobile dislocations and ψ is Taylor orientation factor. In Eq. (9) the mobile dislocation density is considered to be

constant in a certain strain interval. At high strain rates the mobile dislocation density ρ_m changes and the different equation must be used:

$$\dot{\varepsilon} = (1/\psi)\frac{d\rho}{dt} b\, x\,, \qquad (10)$$

where $d\rho/dt$ is the dislocation generation rate and x is the average distance moved by dislocations. Equation (9) is usually used at low or intermediate
strain rates while the equation (10) is more suitable for high strain rates. The sample temperature may be influenced by the experimental conditions. A direct conversion of mechanical work produced during deformation to heat produces an average rise in temperature, ΔT, within a material volume without loss of heat from it. ΔT in the absence of any change in internal energy of the material ($\Delta E = 0$) is obtained as [10]

$$\Delta T = \frac{1}{c_v}\int_0^{\varepsilon_p} \sigma\, d\varepsilon_p\,, \qquad (11)$$

where c_v is the specific heat per unit volume, σ is the applied stress, and ε_p is plastic strain. The strain dependence of the heating is directly proportional to the value of σ.

$$\frac{dT}{d\varepsilon_p} = \frac{\sigma}{c_v} \qquad (12)$$

For the maximum strain rate of 2.427×10^3 s^{-1} the corresponding stress is 150 MPa. With $c_v = 1.85 \times 10^6$ Jm^{-3}K^{-1} for AZ31 alloy a value of $dT/d\varepsilon_p$ = 81 K per unit strain may be calculated. A rise of temperature of a few degrees is obtained for each percent of strain which the material undergoes. This relatively small increase of temperature is due to the averaging and presuming of continuity of the plastic flow process. On the other hand, Armstrong et al. [10] considered only localized rise of temperature which may be followed by the adiabatic shear banding. Such adiabatic forming of shear bands was also used to explain the discontinuous plastic deformation at very low temperatures [11].

TEM showed very high dislocation density in the deformed samples as it is demonstrated in Fig. 6.

The density of dislocations was estimated to be 7–8x 10^{14} m^{-2}. At higher strain rates the waiting time of dislocations at the local obstacles is very small. This may contribute to the formation of dislocation pile–ups. The locally concentrated stress (and therefore plastic work) at the tip of the pile–ups allows reaching a higher local temperature. Strong internal obstacles

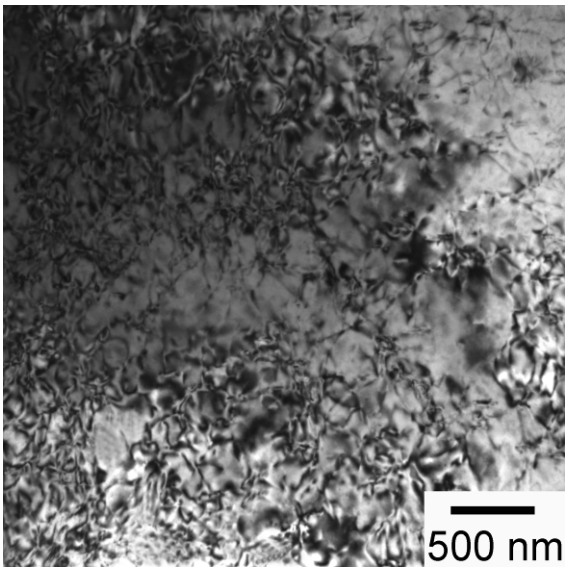

Fig. 6. TEM micrograph of the sample deformed at highest strain rate

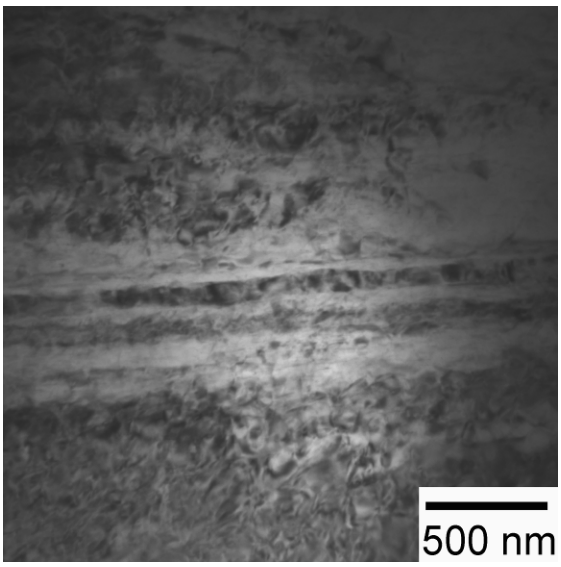

Fig. 7. Massive twins observed in deformed samples

existing in the material can be overcome by the sudden release of pile−ups (or analogous deformation twins or cleavage cracks). Extensive twinning was found almost in all areas of the specimen. Observed twins were of two types. Between massive twins presented in Fig. 7, micro-twins were observed (Fig. 8). The density of these micro-twins increased with increasing strain rate. The adiabatic heating causes also the observed increase of the fracture strain with increasing strain rate in the dynamic tests.

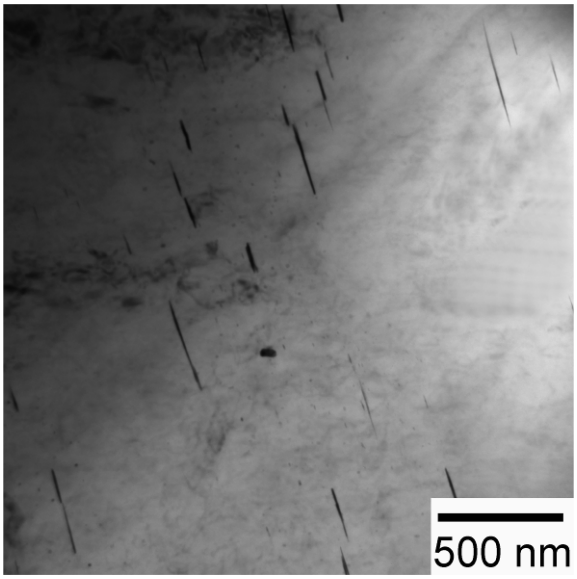

Fig. 8. Micro-twins observed in regions between massive twins

4. Conclusions

The experiments performed using the split Hopkinson pressure bar showed:

- rapid rise of the flow stress at high strain rates;
- rapid increase of the strain rate sensitivity at high strain rates;
- limiting low value of the activation volume (~b^3);
- extremely high dislocation density in deformed samples.

Experiments at high strain rates and the TEM analysis allow us to conclude that the main deformation mechanism at high strain rates is the adiabatic shear banding with the high rates of dislocation and twins formation.

Acknowledgements

This work is a part of the Research Project 1M 2560471601 "Eco-centre for Applied Research of Non-ferrous Metals" that is financed by the Ministry of Education, Youth and Sports of the Czech Republic. The support of the Grant Agency of the Academy of Sciences of the Czech Republic by the Grant Nr. IAA201120902 is also greatly acknowledged.

References

[1] R. Kapoor, J.B. Singh, J.K. Chakravartty: Mater. Sci. Eng. *A 496* (2008) 308-315.

[2] M.A. Meyers, Y.B. Xu, Q. Xue, M.T. Perez-Prado, T.R. McNelley: Acta Mater. *51* (2003) 1307-1325.

[3] G. Dirrasa, A. Ouarem, H. Couque, J. Gubicza, P. Szommer, O. Brinza: Mater. Charact. *62* (2011) 480-487.

[4] M.G. da Silva, K.T. Ramesh: Mater. Sci. Eng. *232* (1997) 11-22.

[5] R.W. Armstrong, S.M. Waley: Inter. Mater. Rev. *53* (2008) 105-128.

[6] U.F. Kocks, A.S. Argon, M.F. Ashby: Progress in Mater. Sci. *19* (1975) 1-207.

[7] 1.G. Regazzoni, U.F. Kocks, P.S. Follansbee: Acta Metall. *35* (1987) 2865-2875.

[8] P.S. Follansbee, G. Regazzoni, U.F. Kocks: Ins. Phys. Conf. Ser. *70* (1984) 71-80.

[9] F.J. Zerilli, R.W. Armstrong: Acta Metall. Mater. *40* (1992) 1803-1808.

[10] R.W. Armstrong, S.C. Coffey, W.I. Elban: Acta Metall. *30* (1982) 2111-2116.

[11] V.I. Startsev: Dislocations in Solids Vol. 6 (Ed. F.R.N. Nabarro) North Holland Publishing Company, Amsterdam- NewYork-Oxford, 1983, pp. 145-233.